

## 8. Nuclei on the neutron-rich side of stability\*

### 8.1. Introduction

The study of nuclei on the neutron-rich side of the valley of stability is an area of research in which great progress has been made since the introduction of large arrays of Compton-suppressed Ge detectors. For such nuclei, production methods at (low-energy) stable beam facilities are limited to deep inelastic, fusion-fission and spontaneous fission. These three classes of reactions have very different characteristics, both in the nuclei produced and in the angular momentum distribution achieved before  $\gamma$ -decay competes with neutron evaporation. Deep-inelastic reactions with heavy ion beams achieve high angular momentum, but are limited to the study of nuclei close to a stable target or beam. These reactions are the primary way to access neutron-rich nuclei with atomic numbers ( $Z$ ) greater than around 65. Spontaneous fission provides the best available method to produce neutron-rich nuclei for  $36 \leq Z \leq 46$  and  $50 \leq Z \leq 64$ , albeit with rather low angular momentum. The fusion-fission reactions lead to the production of a compound system, which already has an appreciable angular momentum, and which due to a reduced barrier fission readily produces fragments with  $I \lesssim 20 \hbar$ . The enhanced excitation energy and angular momentum of the compound system washes out the shell effects that are responsible for asymmetric spontaneous fission and leads to a single-humped yield distribution centered on an atomic number roughly half that of the compound system, thereby filling in the gap in  $Z$  between the heavy and the light fragments distributions of spontaneous fission. In addition, the higher excitation energy and angular momentum of the fragments of fusion-fission reactions promotes neutron evaporation leading to products which are generally closer to stability than those observed following spontaneous fission. The three classes of reactions are clearly complementary, but not exhaustive in the ranges of spin and isospin of the nuclear states produced.

Experiments involving these three reaction mechanisms do share some of the same practical difficulties, namely that in each event there are generally two product nuclei, and, that there are many possible products from any given choice of

---

\* Contribution by A.G. Smith and M.-G. Porquet

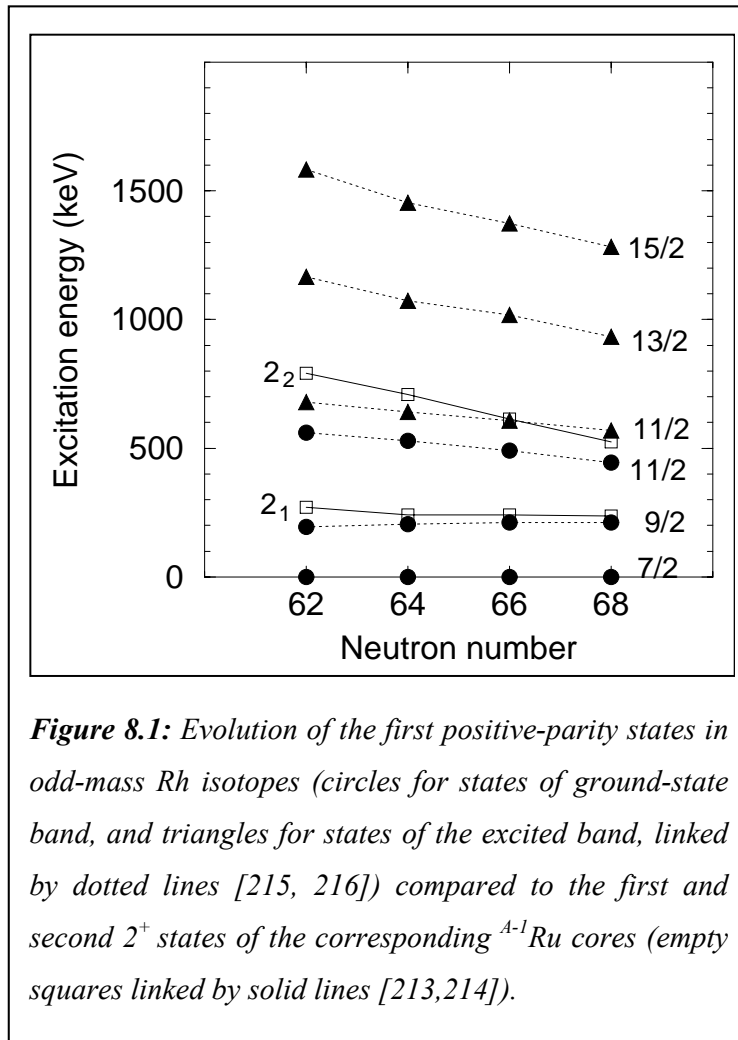
reaction or spontaneously-fissioning source. In fission reactions there is an especially wide range of possible products - typical yields for a given isotope are of the order of 1% of the total. For this reason, the identification of data with a particular fragment requires exceptional selectivity, either through the use of high-fold  $\gamma$  data, where it is a set of energies of coincident  $\gamma$  rays that uniquely identifies the product, or by the direct measurement of  $Z$  and  $A$  of one or both of the products.

## 8.2. Gamma rays from fission fragments

Over the last decade there has been a dramatic increase in the available spectroscopic information relating to neutron-rich nuclei populated in spontaneous and heavy-ion induced fission. This renaissance in fission-fragment spectroscopy has been due primarily to the much increased resolving power of large arrays of germanium detectors. Through improved detection efficiency and high granularity, these arrays have made it possible to obtain reasonable rates for the detection of three coincident  $\gamma$ -rays out of the cascades of multiplicity ten that are typically produced in the decay of the secondary fission fragments (i.e. after neutron emission). In addition to the determination of the energies of excited levels, developments in spectroscopic techniques have allowed for information to be deduced regarding the spins and parities [210] and lifetimes [211] of such states of extreme isospin. EUROBALL has facilitated the continued investigation of the decay properties of fission fragments using established techniques but has also fostered the development of new methods for the measurement of  $g$ -factors and state lifetimes.

### 8.3. Identification of new excited states in fission products

It is a testament to the richness of fission data and to the resolving power of the large Ge-detector arrays that a steady stream of publications containing new level schemes deduced from EUROGAM II experiments continues to complement



the more recent work using EUROBALL. These large data sets, typically containing several times  $10^9$  events of  $\gamma$ -rays emitted from many tens of different fragments, encompass a microcosm of nuclear structure, including collective rotation and vibration, single particle motion, triaxiality and octupole deformation. In this section we take a brief tour of the recent highlights, putting them in the context of work carried out with the earlier phases of the EUROBALL device.

It has been established that, as the neutron number is increased from the valley of stability near  $Z=40$ , the onset of quadrupole deformation occurs. The transition from a spherical to a deformed ground-state shape is sudden for Sr and Zr isotopes, but is gradual for higher  $Z$  nuclei. Furthermore, increasing proton number from  $Z=40$  has the effect of softening the nuclear energy surface to triaxiality. This is evidenced firstly by EUROGAM II measurements that have demonstrated the existence in  $^{106}\text{Mo}$  of a two-phonon vibrational state [212], which shows that  $^{106}\text{Mo}$  is soft to triaxial deformation; and secondly by the energy

levels of the neutron-rich  $^{108,110,112}\text{Ru}$  [213] isotopes, which suggest the presence of a more rigid triaxial shape. Heavy-ion induced fission has been used to populate ruthenium nuclei closer to stability, and evidence for triaxial structures has also been observed in  $^{104,106,108}\text{Ru}$  [214]. In addition, work on the  $Z=45$   $^{107,109}\text{Rh}$  nuclei [215] populated following fusion/fission of  $^{28}\text{Si} + ^{176}\text{Yb}$  has revealed several new rotational structures, two of which can be interpreted within the framework of a particle-triaxial-rotor model. Using yet another fusion reaction  $^{18}\text{O} + ^{208}\text{Pb}$ , which populates heavier isotopes, high spin states of the very neutron rich  $^{111,113}\text{Rh}$  have been recently identified [216]; they exhibit the same behaviour as shown in Figure 8.1.

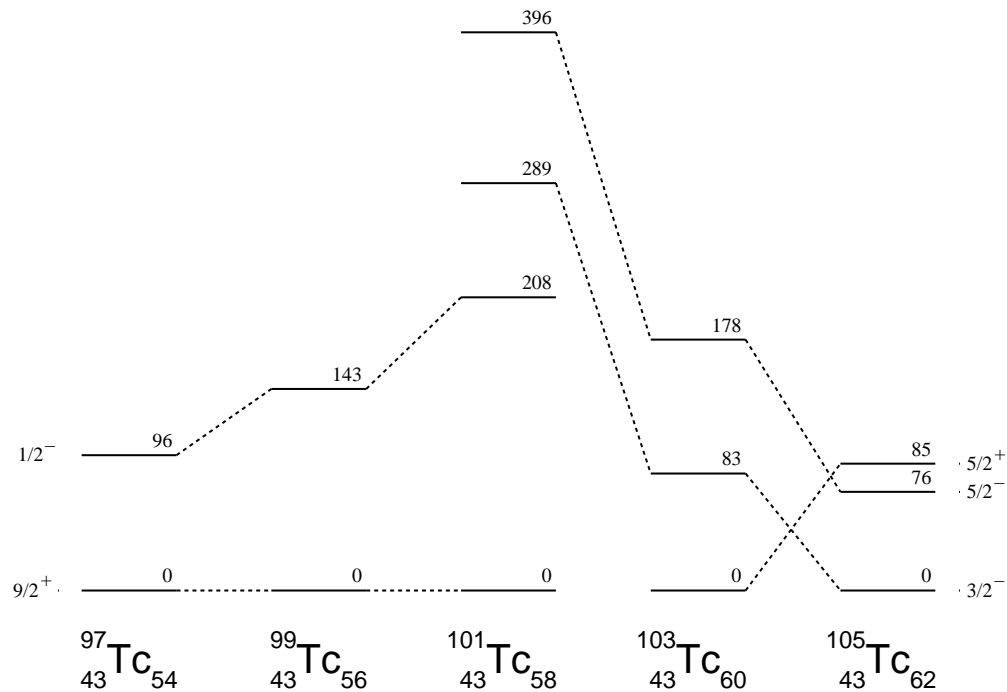


**Figure 8.2:** Evolution of the individual proton states as a function of neutron number in the odd-A  $^{97-105}\text{Tc}$  isotopes [217].

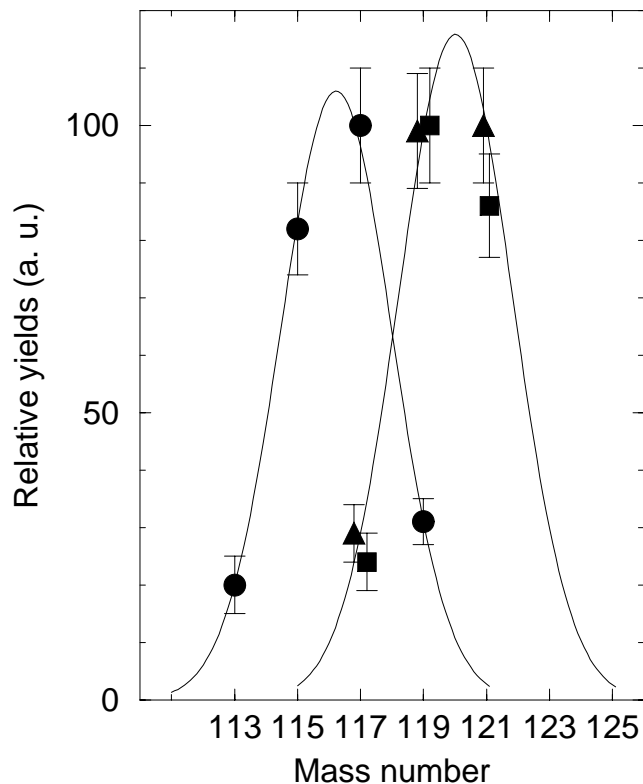


**Figure 8.3:** Yields of the odd- $A$  In nuclei, obtained as secondary fragments from three fusion-fission reactions:

- 90 MeV  $^{12}\text{C}$  on  $^{238}\text{U}$  (triangles)
- 85 MeV  $^{18}\text{O}$  on  $^{208}\text{Pb}$  (squares)
- 152 MeV  $^{31}\text{P}$  on  $^{176}\text{Yb}$  (circles)

The maximum of each experimental distribution has been normalized to 100 (i.e. at  $A = 117$  for the  $^{31}\text{P}$  induced reaction and at  $A = 119$  for the  $^{18}\text{O}$  and  $^{12}\text{C}$  induced reactions). The solid lines show fits with Gaussian distributions [222].

EUROBALL data on fission fragments following the reaction of  $^{37}\text{Cl}$  on  $^{176}\text{Yb}$  has been used to identify high spin states in  $^{103}\text{Tc}$  for the first time [217], and to allow a systematic analysis of the important single particle orbitals as deformation is increased with increasing neutron number (see Figure 8.2). As  $Z$  increases, the triaxial rotation gives way to a quasi-rotational character in the neutron-rich  $^{109,111,112,113,115,118}\text{Pd}$  nuclei, which have been studied in heavy-ion induced fission using EUROBALL ( $^{12}\text{C} + ^{238}\text{U}$  [218]) and earlier with EUROGAM II ( $^{28}\text{Si} + ^{176}\text{Yb}$  [219]). The band structures that are observed in these nuclei show no sign of the sudden shape change that occurs with increasing neutron number in the Zr and Sr isotopes.

The Cd isotopes near stability have long been regarded as good examples of spherical vibrators. Since spontaneous fission gives poor yield for the heavy Cd isotopes, heavy ion induced fission has been used to establish structures based on weakly deformed

configurations in  $^{113-116}\text{Cd}$  [220] and  $^{120,122}\text{Cd}$  [221].

Three different reactions have been used to do a detailed investigation of the Indium isotopes  $^{115,117,119,121}\text{In}$  [222]). The relative yields of In nuclei in these reactions have been deduced from the number of  $\gamma$ -rays populating their ground states (see Figure 8.3). While the  $^{12}\text{C}$  and  $^{18}\text{O}$  induced reactions give similar results, the maximum of the distribution obtained in the  $^{31}\text{P}$  induced reaction is shifted to lower mass number. The use of three different reactions to produce the various In isotopes has turned out to be very efficient to disentangle the coincidence relationships which are often complicated by the existence of many doublets or triplets of transitions very close in energy.

To identify new isomeric states in fission fragments, experiments have also been performed using a fission fragment detector to trigger the EUROBALL array and isolate the delayed  $\gamma$ -ray cascades. The heavy-ion detector, SAPHIR, is made from photovoltaic cells, which can be arranged in several geometries [9]. In the present work [218], it consisted of 32 photovoltaic modules laying in four rings around the target. Fragments escaping from the thin target are stopped in the photovoltaic cells of SAPHIR. The detection of the two fragments in coincidence provides a clean signature of fission events. The EUROBALL time window was  $1\mu\text{s}$ , allowing detection of delayed  $\gamma$ -rays emitted during the de-excitation of isomeric states. Time spectra between fragments and  $\gamma$ -rays have been analysed in order to measure the half-life of isomeric levels. The FWHM of the time distribution for prompt  $\gamma$ -rays was around 15 ns. In this experiment, new isomeric states have been found in  $^{119,121}\text{In}$  nuclei. As an example the level scheme of  $^{119}\text{In}$  and the decay curve of the 152 keV transition depopulating the new  $25/2^+$  isomer is shown in Figure 8.4.

Most of the excited states observed in  $^{115-121}\text{In}$  can be interpreted in terms of a proton  $g_{9/2}$  hole coupled to the Sn core excitations. In addition, intruder bands based on an orbital from the  $\pi[g_{9/2}, d_{7/2}]$  sub shells have been extended up to spin  $19/2 \hbar$ . They behave like the ground state bands of neighbouring Cd isotopes (see Figure 8.5), showing that the shape coexistence phenomenon, well known at low spin in In isotopes, survives at least up to this spin.

Spontaneous fission is an excellent method of populating structures near  $^{132}\text{Sn}$  [223,224], which give important information on the single particle orbitals far from stability. These nuclei delimit the edge of the heavy-fragment bump in the asymmetric yield distribution for spontaneous fission, the peak of which lies near the octupole deformed  $^{144}\text{Ba}$  and

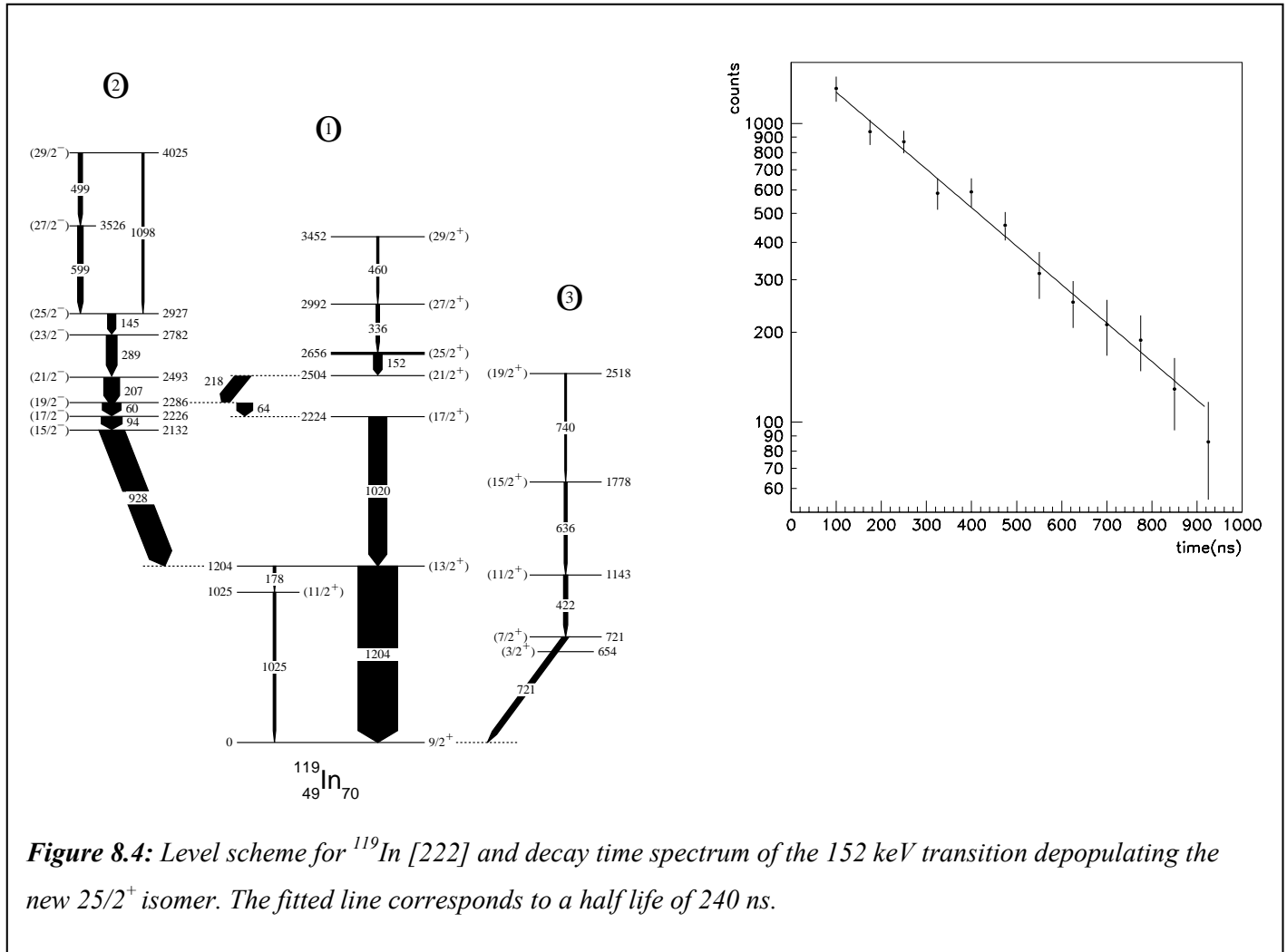


**Figure 8.4:** Level scheme for  $^{119}\text{In}$  [222] and decay time spectrum of the 152 keV transition depopulating the new  $25/2^+$  isomer. The fitted line corresponds to a half life of 240 ns.



which includes the transitional Xenon nuclei [225], and the strongly quadrupole-deformed neutron-rich Ce and Nd isotopes.

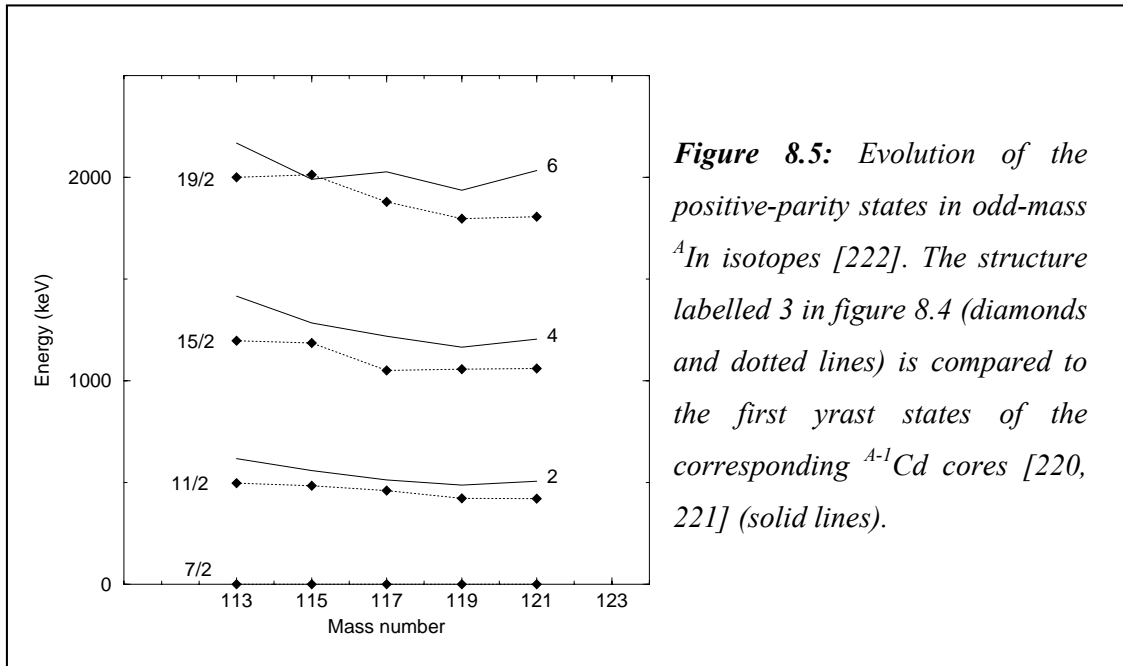


**Figure 8.5:** Evolution of the positive-parity states in odd-mass  $A$ In isotopes [222]. The structure labelled 3 in figure 8.4 (diamonds and dotted lines) is compared to the first yrast states of the corresponding  $A-1$ Cd cores [220, 221] (solid lines).

#### 8.4. Angular correlations, magnetic moments and spin alignment properties

Until very recently, there have been no measurements of the  $g$ -factors of excited states populated in the decay of the secondary fission fragments, although there have been for some time experiments that measure  $g$ -factors of excited states populated in the  $\beta$ -decay of mass-separated fission products.

The advantage of being able to use the secondary-fragment  $\gamma$ -rays, as opposed to those emitted following  $\beta$  decay is two fold. Using the secondary-fragment  $\gamma$ -ray cascades allows access to yrast states up to intermediate spin ( $I \sim 8-16 \hbar$ ) whereas  $\beta$ -delayed  $\gamma$ -rays are generally emitted from states whose spin is close to that of the parent nucleus. In addition, the use of secondary-fragment  $\gamma$ -ray cascades may allow access to more neutron-rich species with shorter  $\beta$ -decay lifetimes. During the EUROBALL III phase, a pioneering experiment [226] was performed to test the possibility of measuring  $g$ -factors of excited states using a spontaneous fission source in conjunction with

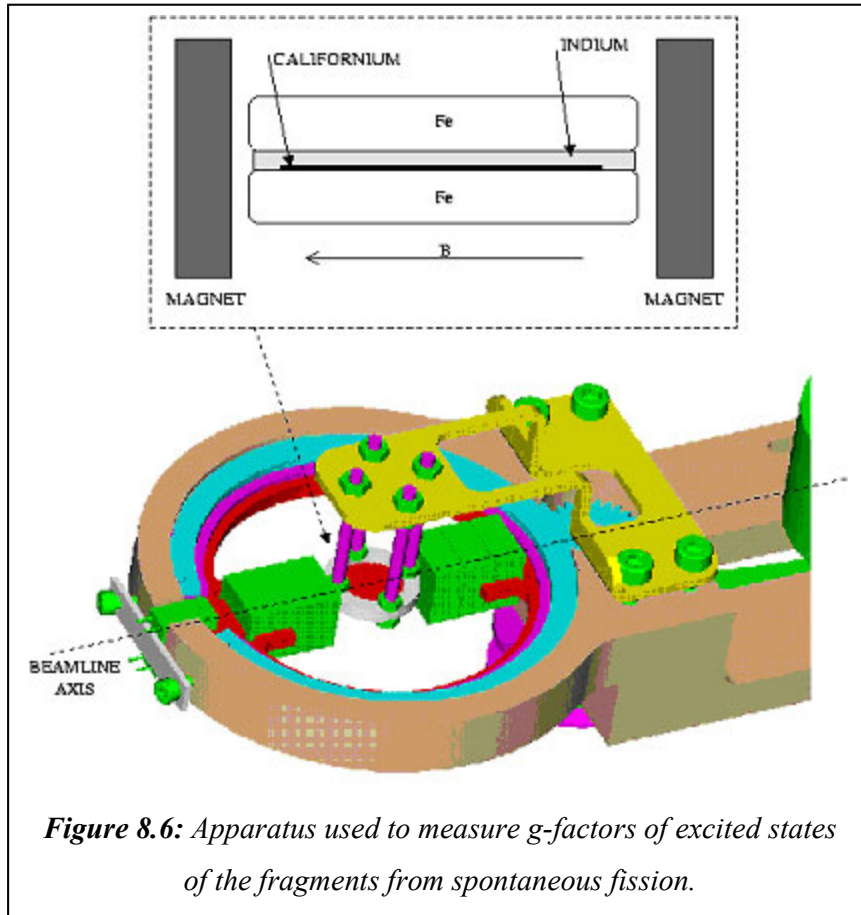
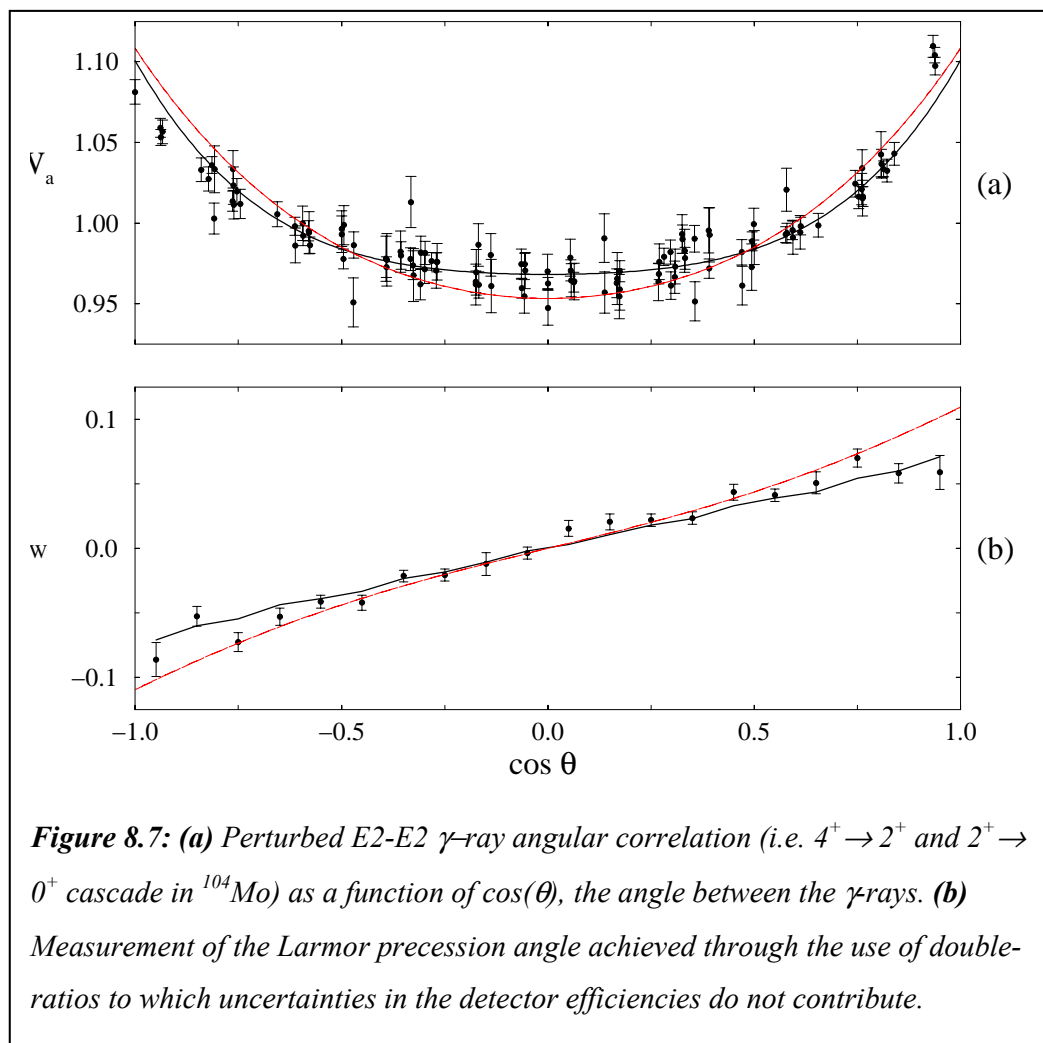


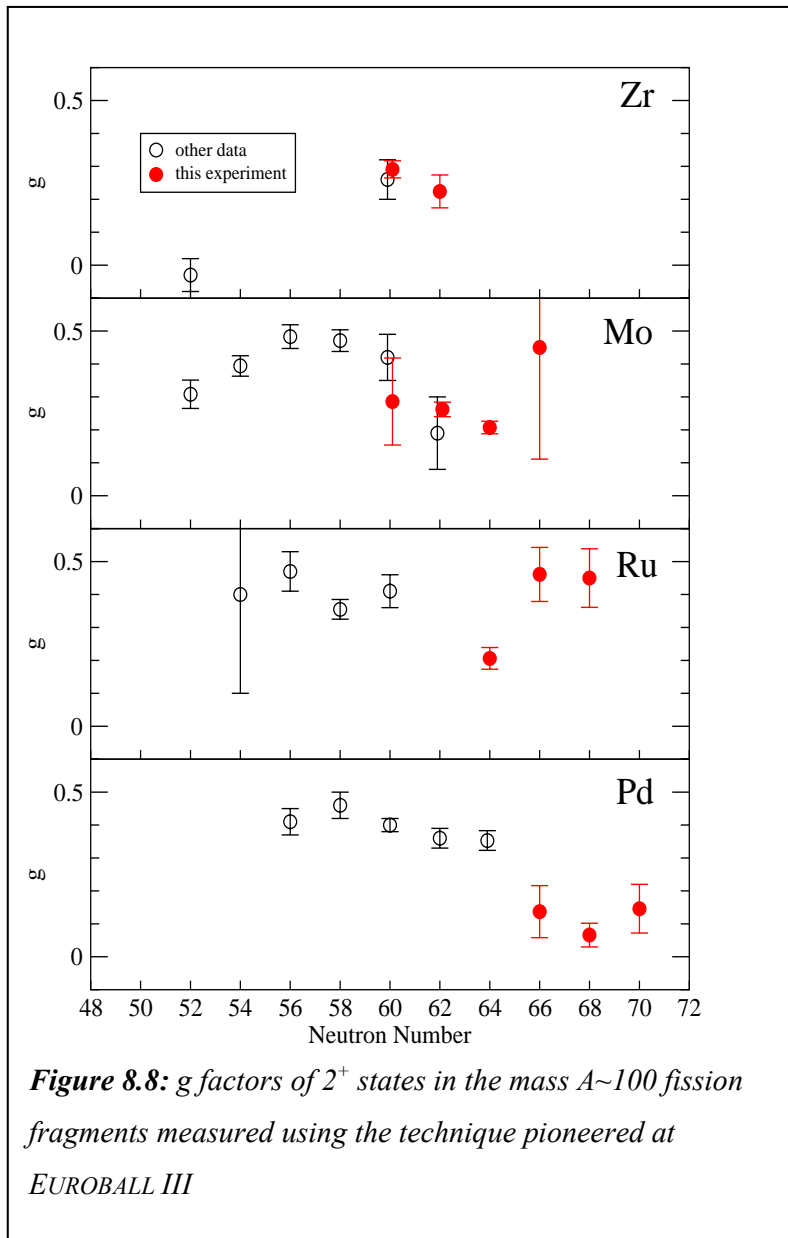
**Figure 8.6:** Apparatus used to measure  $g$ -factors of excited states of the fragments from spontaneous fission.

a large array of Ge detectors. The method involves the direct implantation of the fission fragments into a ferromagnetic host (Gd or Fe) in the form of a thin foil.



As shown in Figure 8.6, the foil is magnetised by a pair of small permanent magnets which can be rotated through  $180^\circ$ . The fission fragments stop in the ferromagnetic host and are exposed to impurity hyperfine fields, which are generally two to three orders of magnitude greater than the applied field of 0.1 Tesla. The impurity hyperfine field causes a Larmor precession of the nuclear magnetic moment, and in so doing cause a perturbation to the  $m$ -substate distributions of any aligned nuclear states. Since in this experiment the fragment direction is not measured, the Larmor precession angle is determined through a careful measurement of perturbed  $\gamma$ - $\gamma$  angular

correlations. An example of such a measurement, for the first  $2^+$  state in  $^{104}\text{Mo}$  is shown in Figure 8.7. This technique has enabled a survey of  $g$ -factors of  $2^+$  states to be made in the  $A \sim 100$  region (see Figure 8.8). The internal angular momentum of the fragments has its origin in dynamical processes that occur in the fissioning system, the so-called



bending and wriggling modes as well as in Coulomb torque immediately following scission. For many years it has been known that the spin of a fragment from spontaneous fission tends to be aligned in a plane perpendicular to the fragment direction, suggesting that twisting modes about the fission axis play at most a minor role in the generation of fission-fragment spins. This conclusion has been drawn from measurements of the angular correlation between the fission axis and the direction of  $\gamma$ -rays emitted in the prompt decay of the excited fragment. Such experiments have been performed with NaI detectors [227] as well as germanium detectors [228].

Recently, a study of the  $\gamma$ -ray decay of low-lying excited states in fragments produced in the spontaneous fission of  $^{252}\text{Cf}$  has revealed a significant correlation between the angles of emission of the  $2^+ \rightarrow 0^+$  transitions of complementary fragment pairs. Calculations of the amount of dealignment that is needed to reproduce the measured  $a_2$  values, and comparison with the results of previous fragment- $\gamma$  angular distribution measurements, suggest that at scission there may be significant

population of  $m \neq 0$  substates associated with the projection of the fragment spin vector on the fission axis (Figure 8.9). Fragments from the spontaneous fission of  $^{248}\text{Cm}$  emit  $2^+ \rightarrow 0^+$   $\gamma$  rays that show markedly reduced inter-fragment correlations, suggesting that either a larger role is played by the relative angular momentum of the fragments, or that the dealignment introduced by the neutron emission and statistical  $\gamma$  decay to the  $2^+$  state is larger in  $^{248}\text{Cm}$  than  $^{252}\text{Cf}$  fission.

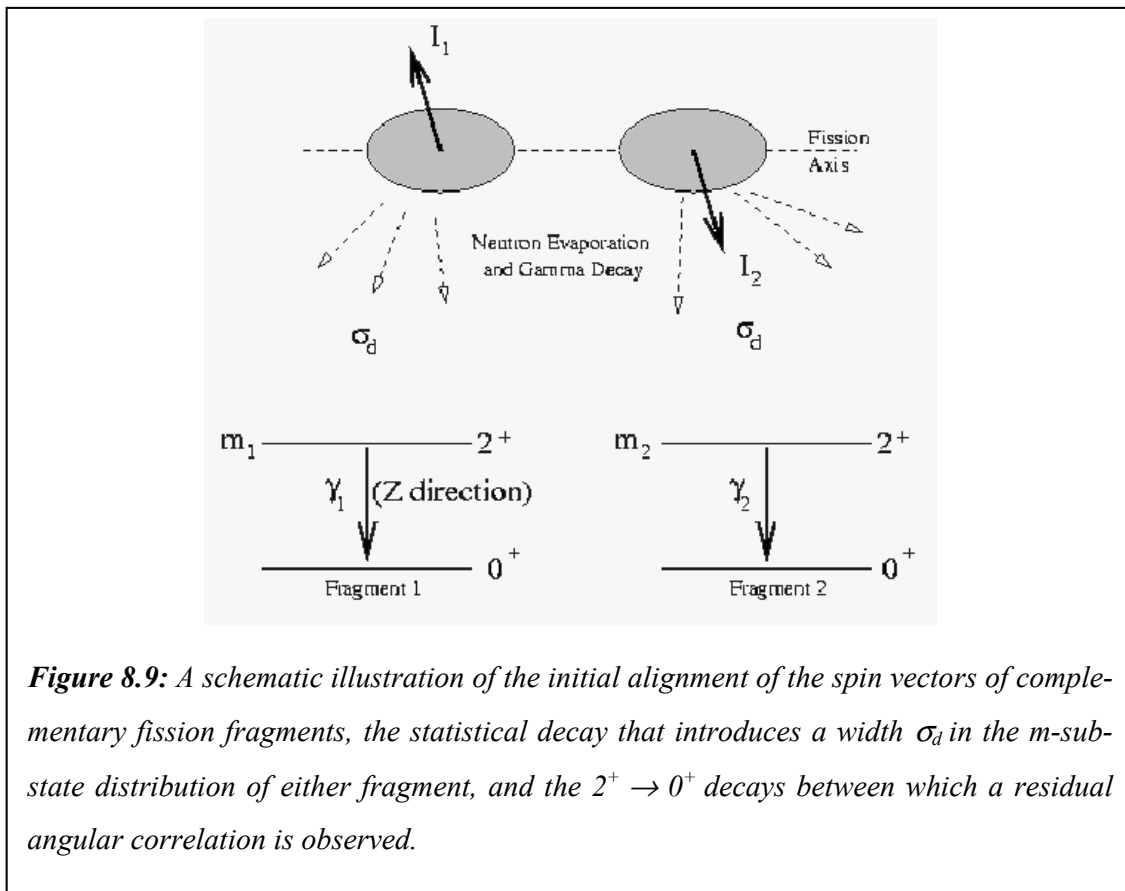


**Figure 8.9:** A schematic illustration of the initial alignment of the spin vectors of complementary fission fragments, the statistical decay that introduces a width  $\sigma_d$  in the  $m$ -substate distribution of either fragment, and the  $2^+ \rightarrow 0^+$  decays between which a residual angular correlation is observed.

### 8.5. Lifetime measurements in fission fragments

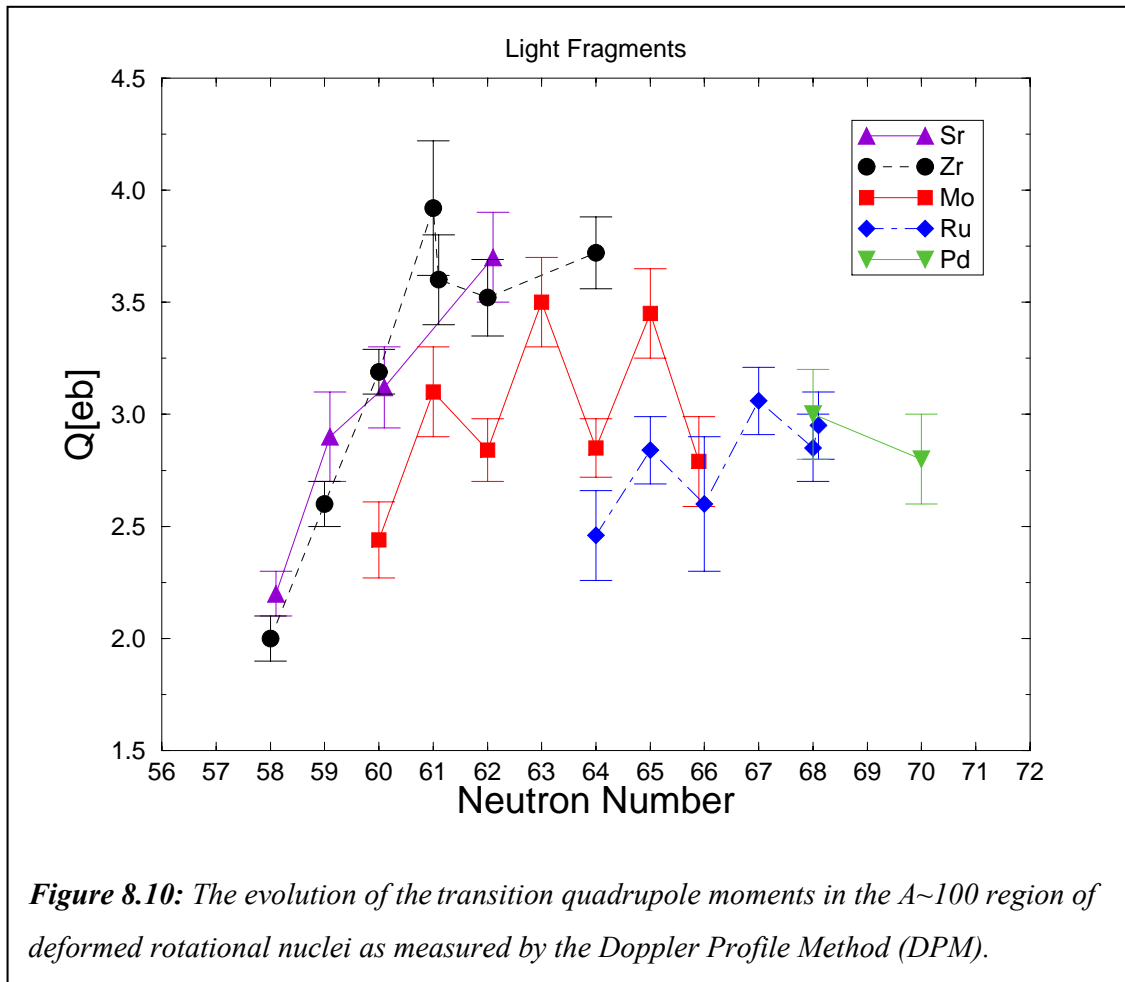
At spins of  $I \sim 10\hbar$ , symmetrically Doppler-broadened lineshapes are observed in the  $\gamma$ -ray energy spectra of many of the light fission fragments from  $^{248}\text{Cm}$  embedded in KCl. The broad lineshapes correspond to decays from states that have lifetimes comparable to (or faster than) the stopping time ( $\sim 1$ - $2$  ps) of the fission fragments in the source pellet, the broadening being due to the variable Doppler-shift that is observed for the time distribution of decays from such states. The Doppler-profile method (DPM) [211,229] combines a simulation of the stopping of the isotropically-directed fission fragment with a simulation of the electromagnetic decay to generate a lineshape that can be compared directly with the data and thereby extract state lifetimes.

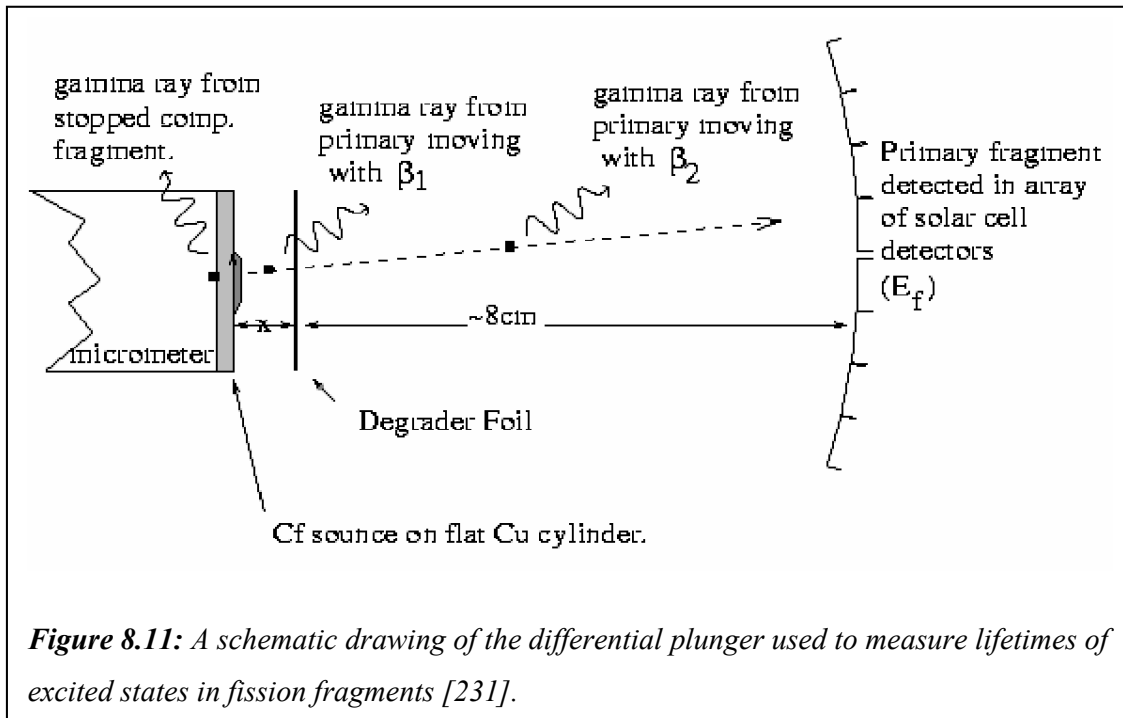
Figure 8.10 shows the quadrupole moments deduced from lifetime measurements for the light fission-fragments at  $I \sim 10\hbar$ . The onset of deformation in the Sr and Zr isotopes is clearly seen to be smooth for these excited states [230], as is the trend to lower quadrupole moments with increasing  $Z$ . The quadrupole moments of the even Mo isotopes are lower than expected, when compared to either predicted ground-state quadrupole moments, or to those deduced from measurements of lifetimes for the first  $2^+$  states. This difference between the quadrupole moments at low and intermediate spin has previously been interpreted in terms of a change in the triaxiality due to  $h_{11/2}$  neutron alignment [229].

In the data presented here, it appears that the quadrupole moments of the odd Mo isotopes show greater stability with increasing spin, having values similar to the Zr isotopes at  $I \sim 10\hbar$ . All of the measurements made in the odd Mo and Ru nuclei correspond to bands of  $h_{11/2}$  character and it may be that the occupation of the moderately prolate-driving  $h_{11/2}$  orbitals by the odd neutron is sufficient to stabilise the axial symmetry. In order to further explore the influence of nuclear rotation on deformation in this region the EUROBALL Fission Fragment Plunger has been constructed [231].

This device, depicted schematically in Figure 8.11 comprises a  $^{252}\text{Cf}$  source on a flat backing, which is mounted on the end of a micrometer. At the centre of EUROBALL IV, a large stretched foil is used to degrade the kinetic energy of fragments emanating from the source. The slowed fragments are then detected in a special configuration of the SAPHIR

array [9] of solar cell detectors. Detection of the in-flight fragment in SAPHIR allows  $\gamma$ -ray energies to be Doppler corrected, either using the full fragment velocity (emission before the foil) or the partial velocity (emission after the foil). Lifetime measurements are made through a comparison of count rates in the fully-shifted and partially-shifted spectral peaks as a function of the source-foil distance. This technique has been proven to have the capability for measurement of lifetimes ranging from a nanosecond to less than a picosecond, and has been used to confirm the decrease with spin of the quadrupole moment of the yrast band of  $^{104}\text{Mo}$ , that was suggested by the DPM data [229].







## 8.6. Gamma spectroscopy with deep inelastic heavy-ion reactions

The excellent resolving power of large Ge detector arrays opened the way to unfold very complex gamma coincidence spectra arising from many nuclei produced in deep-inelastic heavy ion reactions. As a consequence, one can use such processes for the study of yrast structures in nuclei that were hitherto inaccessible in standard fusion evaporation reactions with stable beams. The strong tendency to equalize the  $N/Z$  ratio between the two nuclei colliding at energies significantly above the Coulomb barrier, by appropriate direction of the proton and neutron flow taking place during the collision, gives rise to the production of many nuclei located at the neutron-rich edge of the beta stability line and far beyond it. It has been numerously demonstrated [e.g. 232-,233,234] that, using such reactions, spectroscopy studies could be performed in many neutron-rich nuclei by simple thick target gamma coincidence experiments. Although in such experiments the Doppler broadening might exclude the observation of few gamma rays emitted in flight from short-lived states of recoiling nuclei, the vast majority of important yrast transitions can be detected as discrete gamma lines, since in the populated excitation energy and spin ranges the state life-times and/or feeding times are usually much longer than the stopping time of nuclear products.

The data analysis involves close inspection of gamma coincidence spectra, where, among many families of known transitions arising from the well studied nuclei, one is able to discover new gamma transitions yielding information on yrast structures in nuclei that were previously very poorly known, or even completely unknown. In the latter case special identification procedures are performed by the analysis of gamma cross-coincidences, in which new gamma rays arising from unknown product nucleus are identified by the observation of coincidences with the well known gamma transitions emitted simultaneously from the partner nuclei present in the binary reaction exit channel. In the last decade a number of successful spectroscopic studies of neutron-rich nuclei have been performed, involving also high-spin state studies in the shell model doubly-magic nuclei and their closest neighbourhood. As example one may recall the study of neutron-rich Ni isotopes [235] and observation of subshell closure in the  $^{68}\text{Ni}$  [236], as well as the high-spin state study of the  $^{208}\text{Pb}$

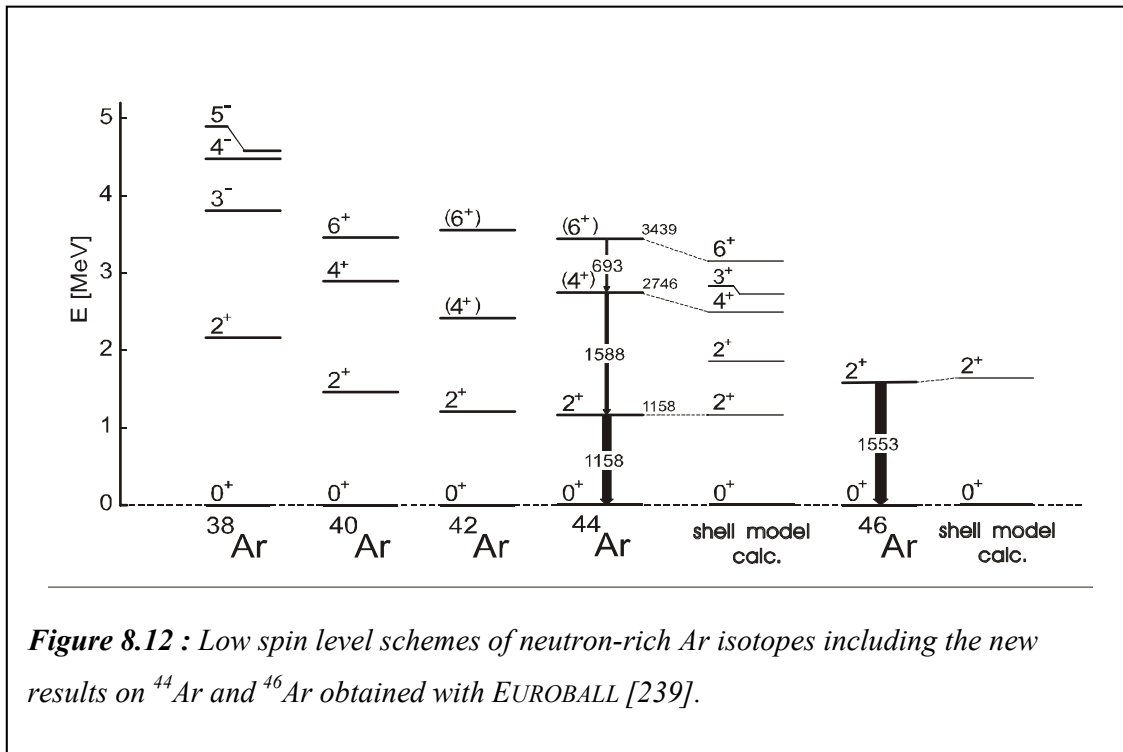


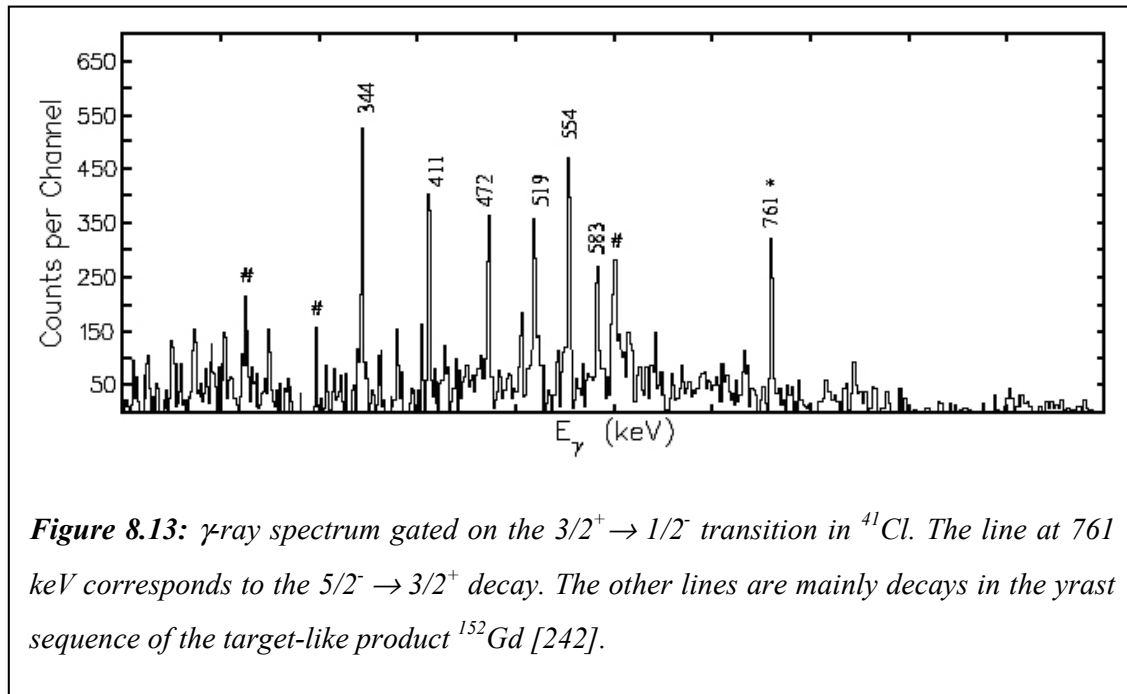
**Figure 8.12** : Low spin level schemes of neutron-rich Ar isotopes including the new results on  $^{44}\text{Ar}$  and  $^{46}\text{Ar}$  obtained with EUROBALL [239].

doubly magic nucleus [237], where recent experiments extended the information to states exceeding the  $I=26$  spin value [238].

The powerful EUROBALL array is a perfectly suited tool for this type of experiments since the available quality and statistics of the gamma coincidence data allows to reach products with very small production cross sections and thereby to access more neutron-rich region of isotopes. However, installation of EUROBALL at accelerators with rather restricted range of energy and mass of available heavy-ion beams, resulted in somewhat limited number of experiments that were devoted to spectroscopic studies with the use of deep-inelastic heavy-ion reactions. Nevertheless, a successful experiment was performed to study neutron-rich nuclei in the region of  $^{48}\text{Ca}$ . A beam of 140 MeV  $^{48}\text{Ca}$  ions from the Tandem accelerator of the Laboratori Nazionali di Legnaro was used to bombard a target of  $0.74 \text{ mg/cm}^2$   $^{48}\text{Ca}$  (backed by 40

mg/cm<sup>2</sup> of evaporated <sup>208</sup>Pb). The gamma-gamma coincidences were collected with the Euroball array. Fusion-evaporation was a main reaction channel, whereas multi-nucleon transfer processes, leading to nuclei from the vicinity of <sup>48</sup>Ca, accounted for less than 1% of the total reaction cross section. Despite this very low production yield, investigation of excited states in some of nuclei around <sup>48</sup>Ca was possible [239]. By examining the cross coincidence relationship between complementary Ar and Ti reaction products one was able to identify in <sup>44</sup>Ar a cascade of gamma rays with energies 1158, 1588 and 693 keV deexciting the yrast states 2<sup>+</sup>, 4<sup>+</sup> and 6<sup>+</sup>, respectively. Also a gamma ray from the first excited state 2<sup>+</sup> to the ground state in <sup>46</sup>Ar, was found at 1553 keV.

These new data on yrast excitations in <sup>44</sup>Ar offer a more stringent test of the large-scale shell model calculations and interactions used. Such calculations were performed for the <sup>44</sup>Ar and <sup>46</sup>Ar nuclei and their results are compared with the experimental findings in Figure 8.12. The agreement is very good for the 2<sup>+</sup> states and satisfactory for higher lying yrast



levels. In  $^{46}\text{Ar}$ , our data confirm the increase of excitation energy of the first  $2^+$  level, which is in line with the persistence of magicity at  $N=28$ . Such phenomenon is indeed predicted by the calculations.

Another example of such a deep inelastic reaction used for spectroscopy with EUROBALL involved the use of a 234 MeV  $^{37}\text{Cl}$  beam on backed  $^{160}\text{Gd}$  target. States in the target-like species  $^{159,160,161,162}\text{Dy}$  [240] have been observed up to spins in excess of  $20\hbar$  and the data interpreted within the framework of cranked shell model and projected shell model calculations. The quasi-neutron  $(v_{i_{13/2}})^2$  crossing in the yrast sequence of  $^{162}\text{Dy}$  is not identified in this work despite being predicted to lie within the observed range of rotational frequencies, and may indicate a larger than expected quadrupole deformation parameter. Spectroscopy has also been performed on the projectile-like species  $^{36}\text{S}$  [241] and  $^{41}\text{Cl}$  [242] (see Figure 8.13). For the first time excited yrast states have been identified in  $^{41}\text{Cl}$  and these have been interpreted as shell model states using an *sdfp* space.

### Acknowledgements

The authors acknowledge valuable contributions to this report by R. Broda, R. Chapman and R. Lucas.